Michigan State University

National Superconducting Cyclotron Laboratory

THE ONE-NEUTRON HALO OF ^{19}C

D. BAZIN, B.A. BROWN, J. BROWN, M. FAUERBACH, M. HELLSTRÖM, S.E. HIRZEBRUCH, J.H. KELLEY, R.A. KRYGER, D.J. MORRISSEY, R. PFAFF, C.F. POWELL, B.M. SHERRILL, and M. THOENNESSEN

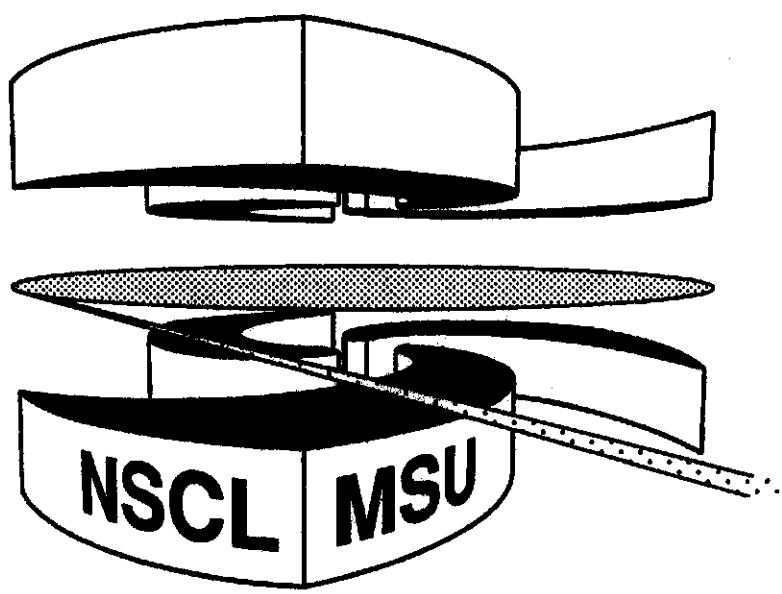

MSUCL-968

MARCH 1995

The one-neutron halo of ^{19}C

D. Basin, B.A. Brown, J. Brown, M. Fauerbach, M. Hellström, S.E. Hirzebruch, J.H. Kelley, R.A. Kryger, D.J. Morrissey, R. Pfaff, C.F. Powell, B.M. Sherrill and M. Thoennessen

National Superconducting *Cyclotron Laboratory,* Michigan *State* University, *Eaet* Lansing, *Michigan 48824*

(February 23, 1995)

Abstract

We have measured the longitudinal momentum distribution of ^{18}C, ^{17}C and ^{16}C after the one-neutron breakup of ^{19}C, ^{18}C and ^{17}C respectively, using the A1200 fragment separator as an energy-lose spectrometer. The observed narrow width of 44.3 ± 5.9 MeV/c for the ^{18}C fragments indicates that ^{19}C is a new example of one-neutron halo, so far the heaviest ever observed. The consequences of the obtained results on the structure of the three isotopes $^{19,18,17}C$ are discussed together with shell model calculations.

PACS numbers : 25.70.Mn, 21.10.Dr, 21.60.Cs, 27.20.+n

Nuclear halos are a new form of nuclear matter which appears in loosely bound systems where the valence wave function extends far beyond the standard nuclear size. Nuclei with this property have recently triggered great interest both experimentally and theoretically [1–3]. The formation of halos originates from the tunneling of one or a few valence nucleon(s) outside the potential. Unlike other kinds of tunneling such as α-decay, the nucleon(s) remain bound to the nucleus. Neutron halos occur in nuclei close to the neutron drip-line, where the valence binding energy approaches zero. Depending on their structure, different nuclei can have a small binding energy for different number of neutrons. Because of the pairing of nucleons, isotopes with an odd number of neutrons are less stable and have small 1n separation energies. This causes the well known odd-even staggering observed in the vicinity of the neutron drip-line, and brings loosely bound nuclei with odd number of neutrons closer to the valley of stability, which makes them more accessible from an experimental point of view.

The only case of a one-neutron halo known so far is ^{11}Be, which has been extensively studied [4–6]. Since its shell structure is well understood and its halo consists of a single neutron, it provides a critical test of halo theories. Here we report the observation of a new example of a one-neutron halo nucleus, ^{19}C. It is the heaviest halo nucleus observed so far, and its study will allow us to further explore the characteristics of the halo phenomenon, in particular in testing the concepts developed for ^{11}Be.

The nucleus ^{19}C is the last bound odd-neutron isotope of carbon. The next case ^{21}C has been observed to be particle-unstable [7]. The measured half-life of ^{19}C is 49 ± 4 ms for β^- decay, which has been observed to be followed by the decay of ^{19}N via γ, one-neutron and two-neutron emission [8]. Its mass has been determined using Time-Of-Flight techniques [9–12], from which a weighted average yields a one-neutron separation energy of $S_n = 242 \pm 95$ keV. This value is significantly lower than the separation energy of ^{11}Be (504 ± 6 keV), suggesting that the halo of ^{19}C should be larger. However, from a simple shell-model picture, the last neutron of ^{19}C should be in the $0d_{5/2}$ orbit, where the ℓ=2 centrifugal barrier would strongly limit the extend of the halo, as shown by recent calculations [13]. We will

see in the following that a shell-model calculation based on the Warburton-Brown effective interaction [14] actually predicts an s-state for the ^{19}C ground state, due to the lowering of the $1s_{1/2}$-orbit. Although the ground state spin/parity assignment of ^{19}C is not known experimentally, it is interesting to note that the intrusion of an s-state as the ground state would be very similar to the case of ^{11}Be for which the same effective interaction correctly predicts the $J^\pi = 1/2^+$ s-wave ground state [15].

An early indication of the loosely bound nature of ^{19}C can be found in its production cross-section from projectile fragmentation. A significant dip compared to the neighbouring nuclei ^{18}C and ^{20}C, was observed (Ref. [7]) in the fragmentation of ^{40}Ar at 44 MeV/u (see fig. 2 of Ref. [7]). The production cross-sections are directly related to the number of bound states in each nucleus via the deexcitation stage of the projectile fragment. The fewer bound states a given nucleus has, the smaller its cross-section is, and a one-neutron halo nucleus would be expected to have few, if any, bound excited states. Moreover, in a recent publication [13], the authors have argued that the formation probability of a halo state, which is related to the probability of having the valence neutron inside the core, scales as R^{-1} where R is the r.m.s radius of the halo [3].

The total cross section of ^{19}C has been measured using a $4\pi - \gamma$ method [16], but with a large uncertainty due to poor statistics. Surprisingly, the value obtained in this experiment ($\sigma_{tot} = 2.7 \pm 1.5$ mb) yields a normal reduced strong absorption radius of $r_0^2 = 1.13 \pm 0.64$ fm^2, deduced using the same procedure as in [16], whereas one would have expected a strong enhancement of this parameter if an extended neutron halo was present. However, as is discussed in [16], the γ detection system used in the experiment had a very low efficiency for detecting forward emitted neutrons, and this was the argument for explaining the much lower reaction cross section found for ^{11}Li than in previous work. The same argument should apply to ^{19}C and the one-neutron breakup cross section would therefore be missed by the detection system due to the strong forward focusing of the neutron. Indeed, a recent extension of a calculation based on the inverse method [17] predicts a strong increase of the matter r.m.s. radius of ^{19}C, which was not observed in Ref. [16].

One of the most direct methods to measure the size of a halo nucleus is by removing the loosely bound particle(s) in a breakup reaction, and measure the momentum of the outgoing fragments. The breakup can result from either Coulomb or nuclear dissociation. Although both reaction channels always coexist, the Coulomb dissociation cross section dominates for heavy targets, whereas it becomes negligible for light targets where the nuclear dissociation cross section is predominant. According to the complementarity principle, the width of the internal momentum distribution of the loosely bound particle(s) is inversely proportional to the spacial extend of the halo.

The early Serber spectator model [18] used plane waves to model both the incoming projectile and outgoing fragment, and found that the differential cross-section is proportional to the internal momentum distribution, which is the Fourier transform of the internal wave function. Unfortunately, this simple picture omits absorption processes which take place between both the spectator and participant part of the projectile and the target [19]. A better formulation using the Glauber approximation shows that the absorption process broadens the momentum distribution, but only in the transverse direction [19]. Final-state Coulomb deflection can also be responsible for a transverse broadening of the momentum distribution. However, the longitudinal momentum distribution remains unaltered by these effects [20], and can be directly related to the internal momentum of the projectile. The measure of the longitudinal momentum distribution of the core after breakup has been successfully used to measure the size of halos in the nuclei ^{11}Li [21] and ^{11}Be [6]. In this experiment, we have measured the longitudinal momentum of the ^{18}C core after the one-neutron breakup of ^{19}C on a Be target.

The secondary beam of ^{19}C was produced from the fragmentation of a 90 MeV/nucleon ^{40}Ar beam on a 470 mg/cm^2 thick Be target. The particles were transported through the A1200 magnetic spectrometer [22] to its second dispersive image plane, where the breakup reaction target was placed. The reaction products were then momentum analysed by the last section of the A1200 where the rigidity was set to the central momentum of the ^{18}C ions coming from the breakup reaction on a 190 mg/cm^2 Be target.

Although the secondary beam had a large energy spread due to the fragmentation process, large enough to fill the momentum acceptance of the spectrometer (3%), it was still possible to achieve a resolution of 0.12% using a dispersion-matched mode [23] in which the momentum dispersion caused by the first section of the A1200 is compensated by the last section. The horizontal position of the particles arriving at the final focal plane was measured using a position-sensitive silicon detector (PSD) which also provided the energy loss measurement. The residual energy was measured in a thick plastic scintillator stop detector located behind the PSD. The Time-of-flight (TOF) from the ^{19}C production target to the final focal plane was measured between the stop detector and the rf-cyclotron signal. The momentum calibration was determined by stepping the rigidity of the last section and measuring the position of ions of known rigidity at the final focal plane.

Although the detected nuclei were dominated by other reactions arising from the much more abundant isotopes of B, Be ,Li and He, the group of events corresponding to the one neutron breakup of ^{19}C could be clearly and uniquely identified because of their unique Time-of-Flight and the specific setting of the magnetic rigidities. The elastically scattered ^{18}C nuclei were suppressed in the last section of the spectrometer because their kinetic energy didn't match the rigidity. Also, their Time-of-Flight was much different from the breakup events, and they could be easily tagged on-line on a Time-of-Flight vs. energy loss spectrum. There was in addition two other groups which could be attributed to the one neutron breakup of ^{18}C and ^{17}C which were also transmitted. These three reactions were observed for the same setting of the spectrometer because of the similarity of the mass ratios and energy losses of the carbon isotopes in the secondary target. The counting rates were 1.7, 8.7 and 3 per hour for ^{19}C, ^{18}C and ^{17}C respectively. The longitudinal momentum distributions observed for the ^{19}C, ^{18}C and ^{17}C breakup are presented in fig. 1. The striking difference between the width of ^{19}C and that of its neighbours ^{18}C and ^{17}C is a clear indication of the halo structure of ^{19}C.

Assuming that the last neutron is in an s orbit, the external wave function can be modeled as an exponential decay (Yukawa) of the form $\exp(-r/\rho)/r$ where the decay length

$\rho = \hbar/\sqrt{2\mu S_n}$ is expressed in terms of the reduced mass μ and the one-neutron separation energy S_n. The Fourier transform of this wave function has a Lorentzian shape $|\tilde{\Psi}(\vec{p})|^2 = \frac{d\vec{p}}{(\hbar^2/\rho^2+\vec{p}^2)^2}$ of width Γ related to the decay length by $\Gamma = 2\hbar/\rho = 2\sqrt{2\mu S_n}$. The r.m.s. radius of the halo is then given by $\langle r^2\rangle^{1/2} = \rho/\sqrt{2}$. As pointed out in [6], the acceptances $\Delta\theta$ and $\Delta\phi$ of the spectrometer change the shape of the Lorentzian momentum distribution. In addition to the determination of the FWHM of the distributions in the lab frame, we have used the Lorentzian-modified line-shape to fit our data and extract the width Γ in the nucleus rest frame. All experimental results and the quantities derived from them are summarized in Table 1. The separation energies for ^{17}C and ^{18}C are extracted from Audi et al. [24].

Since the ^{18}C to ^{17}C distribution is wide, no Γ parameter has been extracted. Instead, we interpret this distribution in the framework of the fragmentation model were the momentum distribution is assumed to be gaussian. The fragmentation model of Friedman [25] relates the width of the parallel momentum distribution to the separation energy as well as an absorptive cutoff radius which, taken as the fragment radius with $r_0 = 1.2$ fm accounts well for ^{12}C and ^{16}O fragmentation [25]. The value we obtain for ^{18}C is 161 MeV/c. Agreement with our measurement is reached if one increases the reduced cutoff radius to $r_0 = 2.0$ fm. This discrepancy might be related to a possible higher neutron density on the nuclear surface (or 'neutron skin') which would alter significantly the one-neutron stripping probability as compared to nuclei on the valley of stability.

A comparison between the r.m.s. radii deduced for ^{19}C and ^{17}C and the radii of the ^{18}C and ^{16}C cores calculated from the constant density law $R = r_0 A^{1/3}$ with $r_0 = 1.12$ fm (2.93 fm and 2.82 fm respectively) shows that the halo of ^{19}C extends far beyond the ^{18}C core, whereas the r.m.s. radius of the last neutron of ^{17}C is of the same order as the size of the ^{16}C core. The one-neutron breakup cross-section follows the same behaviour, as it is significantly larger for ^{19}C than for ^{17}C. This difference should be even more pronounced in the Coulomb dissociation cross-sections, as it has already been seen on ^{11}Li [30] and ^{11}Be [5]. The last column of Table 1 displays the width γ as calculated from the separation energy.

This width is compatible within error bars with the value we deduce from our fit for the ^{19}C data, but is somewhat small in comparison with the ^{17}C data.

Although the spin/parity assignment of the ^{17}C ground state is still unknown experimentally [26], we will see in the following that a shell-model calculation using the same residual interaction [14] that predicts a s-state for the ^{19}C ground state, actually predicts a d-state for the ^{17}C ground state. The effect of angular momentum on the formation of halos recently discussed [13] shows that the r.m.s. radius of the halo diverges as the binding energy goes to zero only for $\ell = 0$ and 1. For $\ell = 2$, the r.m.s. radius increases only slightly and remains finite when S_n goes to 0, as the centrifugal barrier confines the wavefunction close to the potential. Moreover, if the ground state of ^{17}C is a d-state, then the Yukawa approximation can no longer be applied to this nucleus. This picture seems to be consistent with the width we observe, which is smaller than what the Goldhaber fragmentation model predicts, but larger than the one deduced from the very simple s-state neutron halo model.

Relative to a closed-shell configuration for ^{16}O, the minimal shell-model configurations for the neutron-rich C isotopes consist of two-proton holes in the 0p shell and A-14 neutron particles in the 1s-0d shell. The relative position of the $1s_{1/2}$ and $0d_{5/2}$ orbitals is the most essential aspect for the consideration of a 1s neutron halo in ^{19}C. The Millener-Kurath interaction [27] was one of the first to explicitly account for the fact that the $1s_{1/2}$ state comes down in energy as a function of Z from 0.87 MeV above the $0d_{5/2}$ in ^{17}O to 0.74 MeV below the $0d_{5/2}$ in ^{15}C. More recently the 0p-1s0d cross-shell interaction was constrained to reproduce the energies of 165 cross-shell states with potential parameters (WBP) and two-body matrix element parameters (WBT) with a r.m.s. deviation of about 350 keV [14]. These interactions have been used to calculate all measured Gamow-Teller matrix elements for A$\leq$18 [28] with reasonable success, and the calculated Gamow-Teller decay properties of the neutron-rich C isotopes are in excellent agreement with the experimental $T_{1/2}$ and P_n values [29].

The WBP interaction energies relative to ^{14}C for the ground state and low-lying excited states of the C isotopes are shown in Fig. 2 and compared with the experimental ground-state

energies. The overall trend of the theory and experiment match but the theory systematically overbinds compared to experiment, especially for the even-even cases. The experimental level ordering of ^{15}C is well known and is reproduced by the calculation [14]. Spin assignments for the ground state or excited states of ^{17}C are not known, but the calculated [29] vs. experimental $T_{1/2}$ values favor a $3/2^+$ or $5/2^+$ ground-state spin assignment, which would also be consistent with the present experiment. The calculated $T_{1/2}$ values for the $1/2^+$, $3/2^+$ and $5/2^+$ states in ^{19}C are all about the same and thus do not favor any spin assignment. However, the WBP calculation suggests the possibility for a $1/2^+$ spin for the ground state as suggested by this experiment. The calculated spectroscopic factor for removing a $1s_{1/2}$ neutron from the $1/2^+$ state in ^{19}C is 0.58 which is close to the single-particle value and similar to the case of ^{11}Be.

In summary, we have simultaneously measured the longitudinal momentum distributions of ^{18}C, ^{17}C and ^{16}C following the breakup of ^{19}C, ^{18}C and ^{17}C. In the ^{19}C data, both the observation of a narrow momentum peak and a large cross-section indicate the presence a one-neutron halo. This conclusion coincides with a shell-model calculation which predicts an s-state for the ^{19}C ground state. The width observed for the ^{18}C one-neutron breakup has been interpreted in the framework of a fragmentation model and suggests an increase of the absorptive radius cutoff possibly due to a higher neutron density on the nuclear surface. The ^{17}C data also shows a narrow momentum peak, but it is wider and therefore incompatible with the width deduced from the binding energy in the assumption of a s-state neutron halo. Hence ^{17}C may be the first observed case of a 'hindered halo' due to the presence of a $\ell = 2$ centrifugal barrier. Indeed, the shell-model calculation mentioned above predicts a d-state for the ^{17}C ground state, in agreement with this conclusion. More complete data would be most welcome, in particular on the mass of ^{19}C, but also on the one-neutron Coulomb dissociation of these three nuclei ^{17}C, ^{18}C and ^{19}C.

REFERENCES

[1] P.G. Hansen, B. Jonson, Europhys. Lett. **4**, 409 (1987).

[2] T. Kobayashi et al., Phys. Rev. Lett. **60**, 2599 (1988).

[3] P.G. Hansen, Nucl. Phys. A **553**, 89c (1993).

[4] M. Fukuda et al., Phys.Lett. B **268**, 339 (1991)

[5] R. Anne et al., Phys. Lett. B **304**, 55 (1993).

[6] J.H. Kelley et al., Phys. Rev. Lett. in press.

[7] F. Pougheon et al., Europhys.Lett. **2**, 505 (1986).

[8] J.P. Dufour et al., Phys.Lett. B **206**, 195 (1988).

[9] D.J. Vieira et al., Phys. Rev. Lett. **57**, 3253 (1986).

[10] A. Gillibert et al., Phys. Lett. B **192**, 39 (1987).

[11] J.M. Wouters et al., Z.Phys. A **331**, 229 (1988).

[12] N.A. Orr et al., Phys. Lett. B **258**, 29 (1991).

[13] K. Riisager, A.S. Jensen, P. Møller, Nucl.Phys. A **548**, 393 (1992).

[14] E.K. Warburton, B.A. Brown, Phys. Rev. C **46**, 923 (1992).

[15] H. Sagawa, B.A. Brown, H. Esbensen, Phys. Lett. B **309**, 1 (1993).

[16] M.-G. Saint-Laurent et al., Z. Phys. A **332**, 457 (1989).

[17] M. Lassaut, R.J. Lombard, Z. Phys. A **341**, 125 (1992).

[18] R. Serber, Phys. Rev. **72**, 1008 (1947).

[19] M.S. Hussein, K.W. McVoy, Nucl. Phys. A **445**, 124 (1985).

[20] C.A. Bertulani, K.W. McVoy, Phys. Rev. C **46**, 2638 (1992).

[21] N. Orr et al., Phys. Rev. Lett. **69**, 2050 (1992).

[22] B.M. Sherrill, D.J. Morrissey, J.A. Nolen Jr., J.A. Winger, Nucl. Instrum. and Meth. B **56/57**, 1106 (1991).

[23] B.L. Cohen, Rev. Sci. Instrum. **30**, 415 (1959).

[24] G. Audi, A.H. Wapstra, Nucl. Phys. A **565**, 1 (1993).

[25] W.A. Friedman, Phys. Rev. C **27**, 569 (1983).

[26] F. Ajzenberg-Selove, Nucl. Phys. A **460**, 1 (1986).

[27] D.J. Millener and D. Kurath, Nucl. Phys. A **255**, 315 (1975).

[28] W.T. Chou, E.K. Warburton and B.A. Brown, Phys. Rev. C **47**, 163 (1993).

[29] B.A. Brown, unpublished.

[30] B. Blank et al., Nucl. Phys. A **555**, 408 (1993).

FIGURES

FIG. 1. Longitudinal momentum distributions of the recoiling fragment in the one-neutron breakup of ^{19}C, ^{18}C and ^{17}C.

FIG. 2. Calculated interaction energies relative to ^{14}C (lines labeled by the J value) compared to the experimental ground state energies (filled cicles).

TABLES

TABLE I. Summary of experimental results and deduced quantities.

Carbon Isotope	Energy (MeV/u)	FWHM (MeV/c) (lab)	Γ (MeV/c) (rest frame)	$\langle r^2 \rangle^{1/2}$ (fm)	σ_{1n} (mb)	S_n (keV)	Γ from S_n (MeV/c)
19	77.2	44.3±5.9	46.9±8.8	6.0±0.9	105±17	242±95	41±12
18	86.2	110.3±12.4			34.8±2.1	4180±30	
17	96.8	82.5±15.9	94±19	3.0±0.6	40.9±4.3	729±18	71.5±0.9

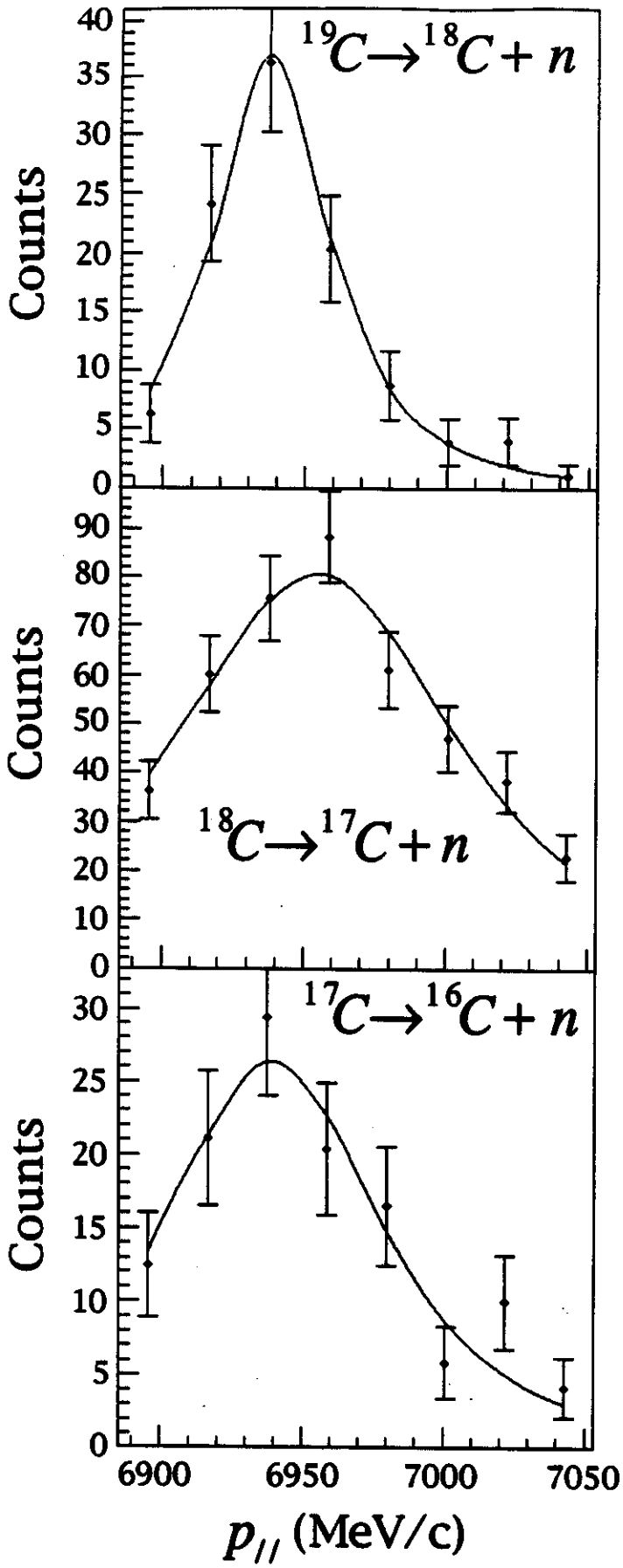
$^{19}C \rightarrow {}^{18}C + n$
$^{18}C \rightarrow {}^{17}C + n$
$^{17}C \rightarrow {}^{16}C + n$
Counts
Counts
Counts
6900
6950
7000
7050
$p_{//}$ (MeV/c)

Fig. 1

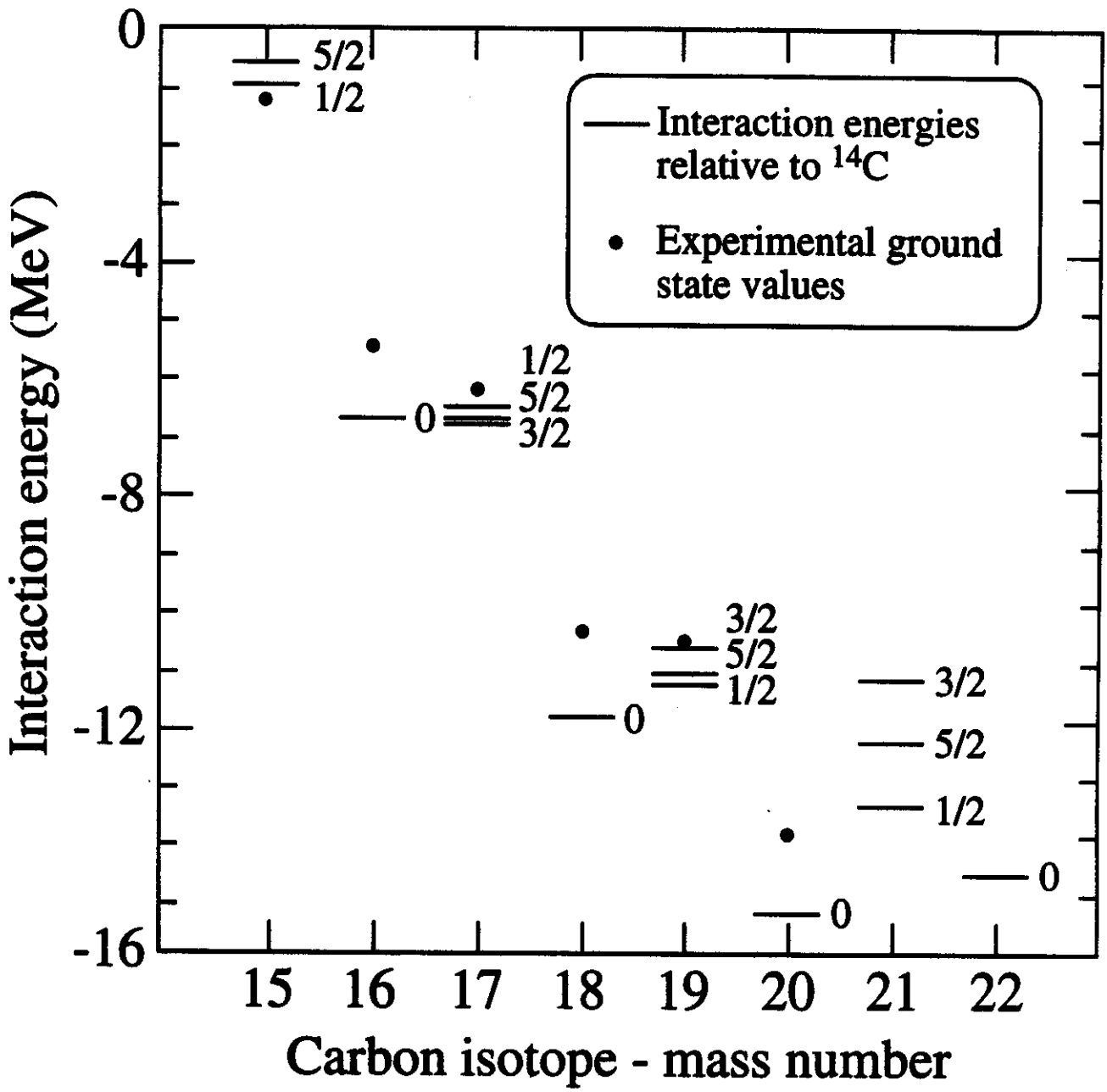
0
-4
-8
-12
-16
Interaction energy (MeV)
15
16
17
18
19
20
21
22
Carbon isotope - mass number
Interaction energies relative to ^{14}C
Experimental ground state values
5/2
1/2
0
1/2
5/2
3/2
0
3/2
5/2
1/2
0
3/2
5/2
1/2
0

Fig. 2